RESEARCH ARTICLE

Riparian vegetation life stages control the impact of flood sequencing in a laboratory braided river

Rocio L. Fernandez[1] | Stuart McLelland[2] | Daniel R. Parsons[2] | Bas Bodewes[1]

[1] Department of Geography, Geology and Environment, University of Hull, Hull, United Kingdom

[2] Energy and Environment Institute, University of Hull, Hull, United Kingdom

Correspondence

Rocio Luz Fernandez, Department of Geography, Geology and Environment, University of Hull, Cottingham Rd, Hull HU6 7RX, United Kingdom. Phone: +44 (0)7380409490.

E-mail: r.l.fernandez@hull.ac.uk

Abstract

With river flooding being more frequent due to climate change, the interaction between fluvial morphodynamics and riparian vegetation may depend in part on the sequence of flood events. This paper describes a laboratory study of the geomorphic adjustment of a braided river to flood sequencing at five different strengths of riparian vegetation. By using alfalfa as a proxy for the braidplain vegetation, differing plant life stages were used to represent the varying strengths of biogeomorphic feedbacks. Sediment flux conditions included runs with both

equilibrium sediment loads and deficit loads. Changes in bed topography were assessed by using a detailed digital elevation model, digital imagery and continuous monitoring of the transported sediment. The results broadly demonstrate that in absence of plant colonisation, riparian vegetation encouraged the development of new channels, increased the system channel width and enhanced topographic irregularity, these effects being more noticeable during the low-flow periods. The morphologic changes were however less sensitive to variations in discharge as the vegetation influence (size) increased from minimum to maximum, until vegetation began to die back and the impacts of flood sequence became yet again evident. Although the sediment transport rate was effectively reduced under full-grown vegetation conditions, the presence of the mature plants across the braid bars resulted in the greatest channel scour depths. Overall, in absence of plant colonisation, the below-ground biomass played a more significant role in river response to flow variability as compared to the above-ground biomass.

KEYWORDS

braided river, vegetation, flood sequence, climate change, biogeomorphology

1 | INTRODUCTION

Flood frequency and magnitude are expected to increase over large parts of the world due to climate change (IPCC, 2014) and the interaction between fluvial morphodynamics and riparian vegetation may be thus influenced by the ordering of flood events as the frequency of flood flows increases. In other words, the

influence of the non-constant forcing discharge, or the impact of the antecedent flood (either low or high flood), might become more significant in driving the evolution and change in fluvial environments.

Experimental models, in the context of floodplain evolution over long periods of time (e.g. decades) typically use a magnitude-frequency approach, in which the experiments simulate just the significant flood events and ignore periods when flows have little or no competence to transport sediments and affect morphodynamics. This enables additional time-scale compression by increasing the geomorphological work completed in a period of model time (e.g. Peakall *et al.*, 1996). A rigorous specification of long-term sequencing of flood events of different magnitudes and its simultaneous interaction with riparian vegetation has been lacking, despite the critical importance that it may have particularly in dynamics river systems that experience high erosion/deposition rates, and are thus more sensitive to a change in the flow regime. In this context, the sequential characterization of channel change in relation to discharge fluctuations is thus essential to understand the effect of temporal ordering of flood events on channel behaviour when modelling river response over long time scales.

Flow variability is known to impact braided planforms more than single thread systems because braided rivers are characterized by higher width/depth ratios and they are strongly dependent on the exposure of bar-scale topography (Bridge, 1993; Tal *et al.*, 2004). Indeed, the braiding pattern in some rivers can change radically, acting as a single channel at bankfull stage and only espousing a characteristic braided appearance on the falling stage (Bristow & Best, 1993). Vegetation interactions can also rapidly change braided rivers with scour-induced

channel narrowing in response to large flood events being stabilised by subsequent vegetation encroachment resulting in lower width/depth ratios (Johnson, 1994; Piégay *et al*., 2009; Toone *et al*., 2014). A clear example is Waitaki river in New Zealand, where less frequent floods over a period of 70 years resulted in reduced braiding intensity due to vegetation encroachment (Hoyle *et al*., 2012). This effect of riparian vegetation on fluvial landform development has been identified as an engineering function of the plants (Naiman *et al*., 1999; Piégay & Gurnell, 1997; Gurnell & Pett, 2006) leading to the concept of biogeomorphic succession (Corenblit *et al*., 2007, 2009, 2014), in which four stages can be identified based on the relation between resisting and destructive (floods) forces (Bätz, 2016). The first two stages (seedling dispersion by flow and survival) are geomorphological, with the vegetation being highly exposed to the physical environment. During the third stage, the bio-geomorphological period, the interaction between plants and their physical environment is highest, and plants are able to resist total destruction by flow. During this stage, deposits are more resistant to erosion as roots have increased bed sediment cohesiveness and fine sediment trapping is enhanced via the aboveground biomass. The fourth stage is the ecological stage, in which vegetation becomes independent of fluvial processes and obtains their resource demands (nutrient and water retention) through autogenic processes.

This engineering role of vegetation, with the regression or progression in time and space of the plants, has prompted a number of laboratory investigations that have shown that vegetation can occupy newly exposed areas of bare sediment leading the river flow to focus into a single main channel (Gran & Paola,

2001; Tal & Paola, 2007, 2010) or induce bifurcation and braiding when single large plants are present (Coulthard 2006, Van Dijk *et al*., 2013). Several field studies have also documented that colonisation by vegetation is not easily reversible and therefore typically has long-term impacts on the riverbed; however, vegetation can only colonise the riverbed up to a critical threshold of flooding frequency and magnitude, since vegetation colonisation can be restricted by different factors like vegetation removal due to destructive floods or inundation exceeding the plant's tolerance (Johnson *et al*., 1985, Gurnell & Petts, 2006, Crouzy *et al*., 2012, Bätz, 2016). Also, the duration of droughts can affect vegetation regeneration. Hence, Garsen *et al*. (2014) linked a drought duration of approximately >30 days to a strong reduction of riparian biomass and stated that high drought intensities can damage riparian seedling survival.

To address the impacts of increased frequency of flood flows, it is crucial to develop a further understanding on how channel morphodynamics and riparian vegetation are linked in a regime where colonisation rates by riparian vegetation are insignificant due to the frequency of flood events. This suggests that it is important to get a better understanding of river evolution when the ratio $T_{veg} / T_{flood} > 1$, where T_{veg} is the biological timescale (the time required for vegetation colonisation which is associated to plant germination and development rates) and T_{flood} is the hydrological timescale (the arrival time of floods), as reported in Paola (2001). Under this condition, two main issues arise that need further consideration; first, as flood flows become more frequent, how does flow variability impact on river morphodynamics over a sequence of events. Second, the higher frequency of the flood events will likely remove any young vegetation and colonisation will not take

place, but existing vegetation (or the fraction of vegetation cover that was not removed by a previous flood) will continue to grow by increasing the chances to survive the following floods. In this respect, when surviving vegetation grows beyond the uprooting capacity of the following flood event, and colonisation by vegetation is not allowed, only the influence of the established vegetation it is expected to remain over time.

This research develops new experimental protocols to simulate flood sequences from a combination of low and moderate flood flows comparable to 2 or 5 year flood events (high recurrence period) and variable growth stages of established plants. The study determines the importance of flood sequencing in controlling river morphodynamics in absence of plant colonisation, and provides insights into how different stages of plant growth influence flow and solid transport along the river reaches as well as drought conditions. Results are invaluable for understanding morphological change-braidplain vegetation feedbacks in long-term evolution modelling that often do not consider the influence of flood sequencing.

2 | METHODS

2.1 | Experimental setup and procedure

The experiments were conducted in the Total Environment Simulator facility (TES), University of Hull. The TES was divided into two mobile-bed flume channels, each functioning as an individual channel of 2.5 m wide and 10 m long, but both channels were similar to each other what allowed the repeatability of results. A schematic view of the experimental setup is shown in Figure 1, and a summary of the experimental conditions is given in Table 1. Each experiment was initialised

with a longitudinal bed slope of 0.015 m/m set by grading a ~10 cm thick sand bed (d_s = d_{50} = 0.45 mm). The slope remained almost constant throughout the experiments. Flow was introduced through a small box partly filled with cobbles and located at the upstream end of each flume to reduce inflow turbulence from the pump. Above the inlet boxes, a sediment feeder released sand, with the same grain size characteristics as the original bed, at a constant rate. During each experiment the discharge, the bed load input and the bed load output (captured in a sediment trap at the downstream end of each flume) were measured continuously.

Prior to the experiments described herein, a long duration experiment with constant-discharge was completed to characterise a steady-state, self-formed braided channel morphology and establish the transport rates for the simulated flood events. This early experiment was started from a flat, sloping bed with a small channel carved into the middle in order to accelerate the initial stage of braid channel development. A constant inlet flow discharge of Q = 1.5 L/s and sediment input rate Q_s = 6 g/s was maintained for approximately 40 hours. The resulting braided channel morphology was then used as the initial morphology to calibrate the discharges and sediment loads for the two flows to be used for the flood sequence events. The initial sediment feed rates were estimated empirically (e.g. Meyer, Peter and Muller, 1948), and then adjusted to maintain the bed slope at the initial value of 0.015 m/m, to ensure there was no net aggradation or degradation during the simulated flood events under equilibrium conditions. From these tests, a discharge of Q = 2 L/s was selected for the low flood event, with an associated sediment feed rate of Q_s = 8.0 g/s (Table 1). The high flood was produced using Q

= 3 L/s and a sediment feed rate of Q_s = 15.5 g/s, and it was the highest flow possible without submerging the bed from wall to wall. A second low flood event (Q = 2 L/s) but now with the sediment feed rate reduced to 80% (Q_s =1.6 g/s) was further considered to simulate a low bed load input in one of the rivers (Flume 1), to model the case where sediment transport capacity exceeded supply (called herein as a deficit flood).

After the flow and sediment discharge conditions were calibrated, the two main experiments were carried out. These experiments were similar to each other, but the first experiment was completed with un-vegetated braidplains (*Experiment I*) as a control experiment, whilst the second experiment had vegetated braidplains with different growth stages of established plants (*Experiment II*). These two experiments (with un-vegetated and vegetated braidplains) were run twice, once in each flume, to allow the repeatability of results.

For each experiment, following the development of a steady-state braided morphology using constant flow and sediment discharge (as described above), the system was subjected to a succession of a stepwise-variable flood events that included a combination of the simulated low and high magnitude flood events. Each flood event, here termed also a run, lasted 1 hour to allow significant morphological change (>30% of the total planform area as estimated during the initial calibration tests), and the floods were continuously repeated in order to study how the system evolved over a period comprising 12 floods in *Experiment I* and 18 floods in *Experiment II*. The experiment with vegetation (*Experiment II*) was longer as it included different plant life stages.

During each experiment, the bed topography was surveyed, in a dry state, between each flood event with an overhead 3D terrestrial laser scanner (Faro Focus X330); this DEM data was then derived over a 1 mm grid resolution. Additionally, six remotely controlled, overhead cameras were used to capture time-lapse images at intervals of between 1 and 60 seconds during the flood events.

For *Experiment II*, after developing the initial, steady-state braided morphology, alfalfa seeds (*Medicago sativa*) were uniformly spread by hand over the bed with a spatial density of 1 seed/cm^2. To prevent plant growing within channels, seeds from the channelized areas were removed by briefly running low flows (Q = 0.8 L/s) after seeding. Four different growth periods were investigated (4, 8, 14 and 20 days) here termed stages I, II, III and IV, along with a dying stage V, to gain insights into the relative role of the plant's age (size) in the geomorphic impact of the sequential floods. Figure 2 shows the sequence of runs (Figure 2a), together with the characteristic (average) lengths for the vegetation during the different stages considered (Figure 2b-2c). As there was not reseeding between runs, the size of the plants remained uniform along the planform area during the experiment. An overhead view of different vegetation patterns during *Experiment II* is shown in Figure 3. During the experiments there was no interflow between runs, but the water table was maintained during the growing period using a groundwater flow input. Regarding the seeding, the spread of seeds was done in two opportunities; at the start of Stage I, and also at the end of this stage to be able to continue with the experiments (i.e. with the second growth stage) as there was not plant left on the braid bars after Run 4. Note that there was not reseeding between floods in the way to allow the vegetation to progress along the bed during interflows. Hence, the

experimental procedure did not include a period of vegetation or morphological recovery between the runs. This procedure was adopted since the goal was to model the situation where the subsequent flood event occurred before the system had fully recovered from the previous perturbation and vegetation colonisation was not able to take place due to the high frequency of the floods. In this respect, the changes (if noticeable) in vegetation cover from run to run during *Experiment II*, shown in Figure 3, were purely caused by removal of existing vegetation by erosion. The final panel (f) in Figure 3 corresponds to the dying stage (Stage 5) performed to the end of the experiment to simulate the conditions of drought or situations where vegetation dies due to desiccation in arid environments.

Table 1 Experimental flow and sediment discharges used in both *Experiment I* (bared braidplain) and *Experiment II* (vegetated braidplain). Q* refers to the nondimensional flow discharge computed as $Q^* = Q/\sqrt{g}d_s^{5/2}$

	Q (L/s)	**Q_s (g/s)**	**Duration**	**Q***
Forming discharge	1.5	6	continuous	$11.1\ 10^4$
Low flood	2	8	1 hour	$14.9\ 10^4$
High flood	3	15.5	1 hour	$22.3\ 10^4$
Deficit flood	2	1.6	1 hour	$14.9\ 10^4$

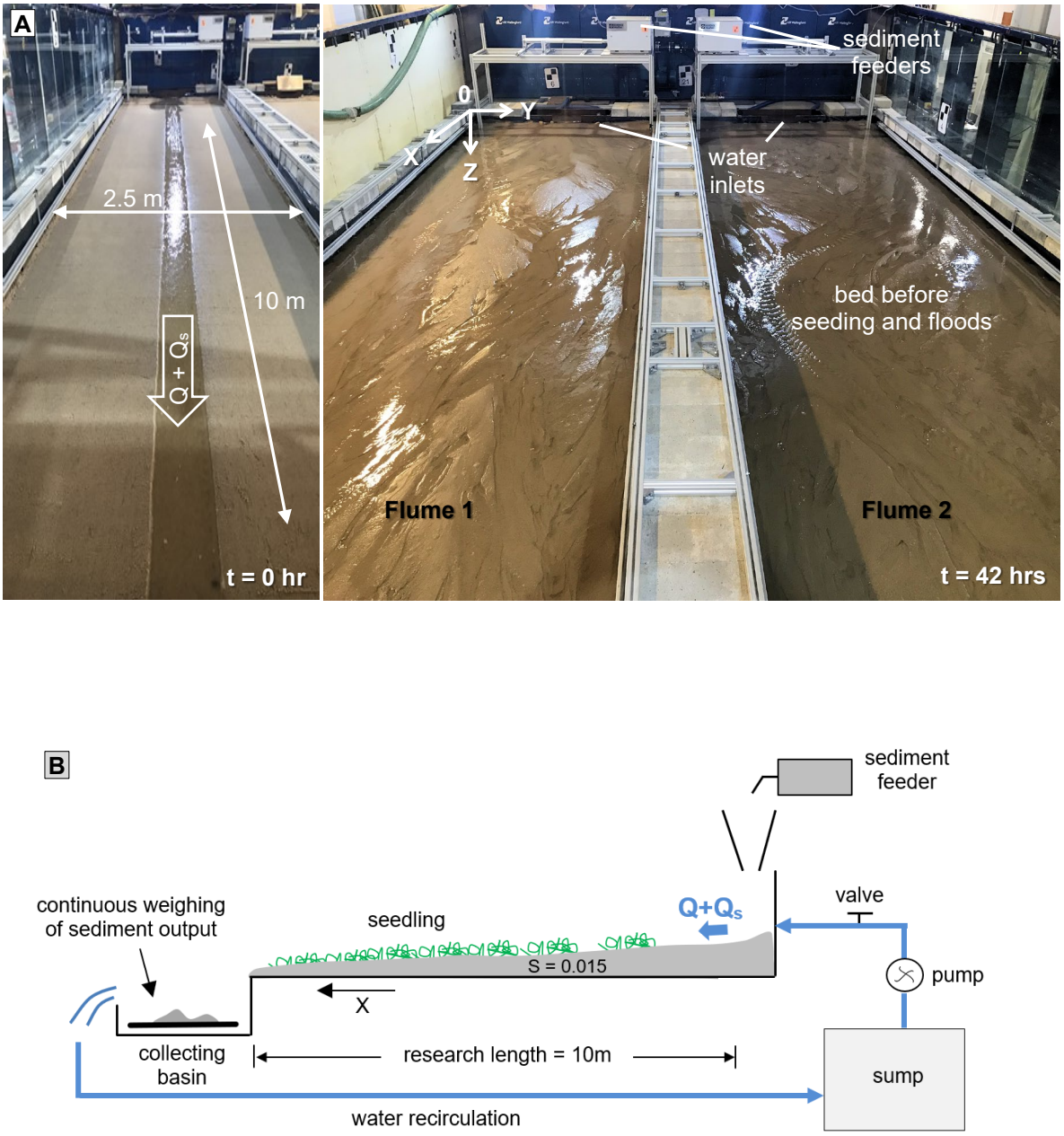

Figure 1 Experimental flume set-up. **a)** Overview photographs of the Total Environmental Simulator facility at the initial time of *Experiment I*, t = 0 hour (left), and after reaching a stable bed condition, t = 42 hours (right). **b)** Schematic side view of the setup. The working length was filled with uniform quartz sand and bed slope of 0.015. Sediment was collected and weighted at the downstream end of the channel during the experiments.

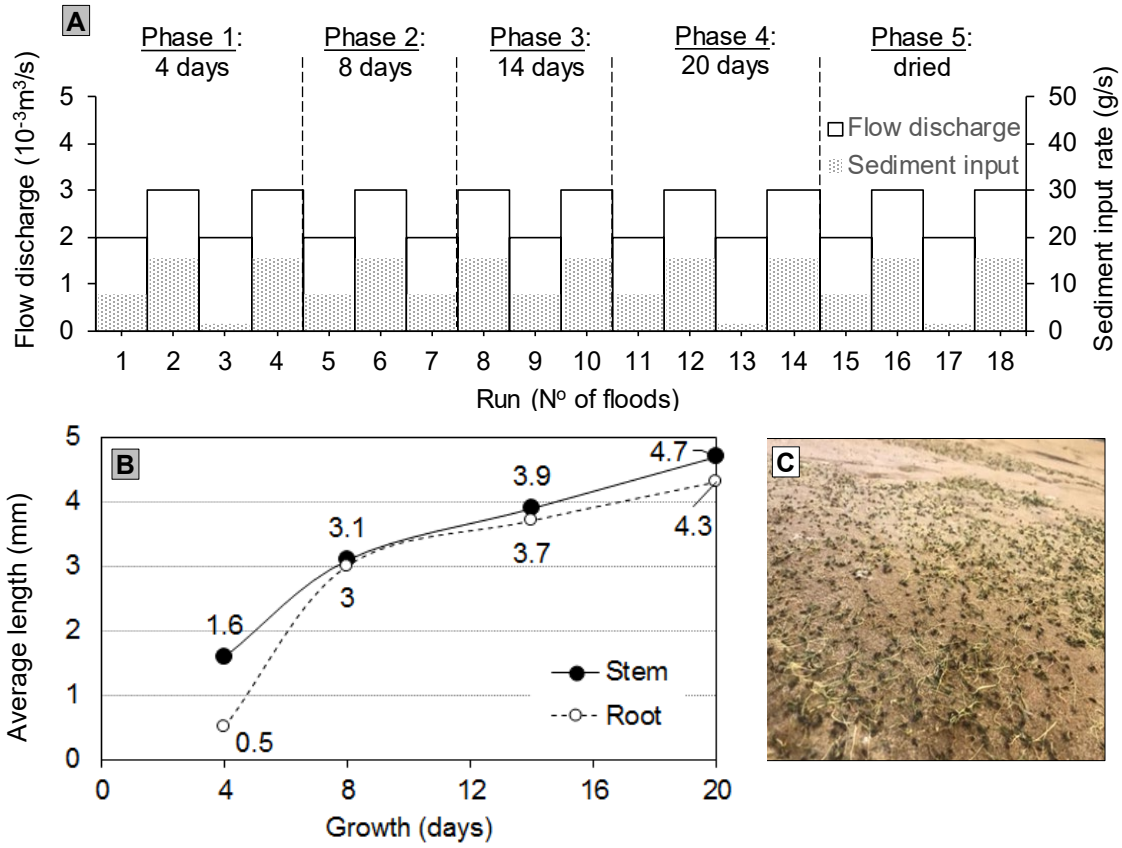

Figure 2 *Experiment II*. **a)** Sequence of the 18 runs (or flood events) during the five stages of alfalfa growth (4, 8, 14 and 20 days and dried stage). Each flood event lasted 1 hour. Three of the floods in Flume 1 (Runs 3, 13 and 17) were released with a deficit in sediment within the inflow, while the same flood sequence without deficit runs was released in Flume 2. **b)** Average growth curves for the root and stem lengths of the alfalfa sprouts (Stages 1-4). **c)** View of the dying conditions of the alfalfa used in Stage 5 in both flumes.

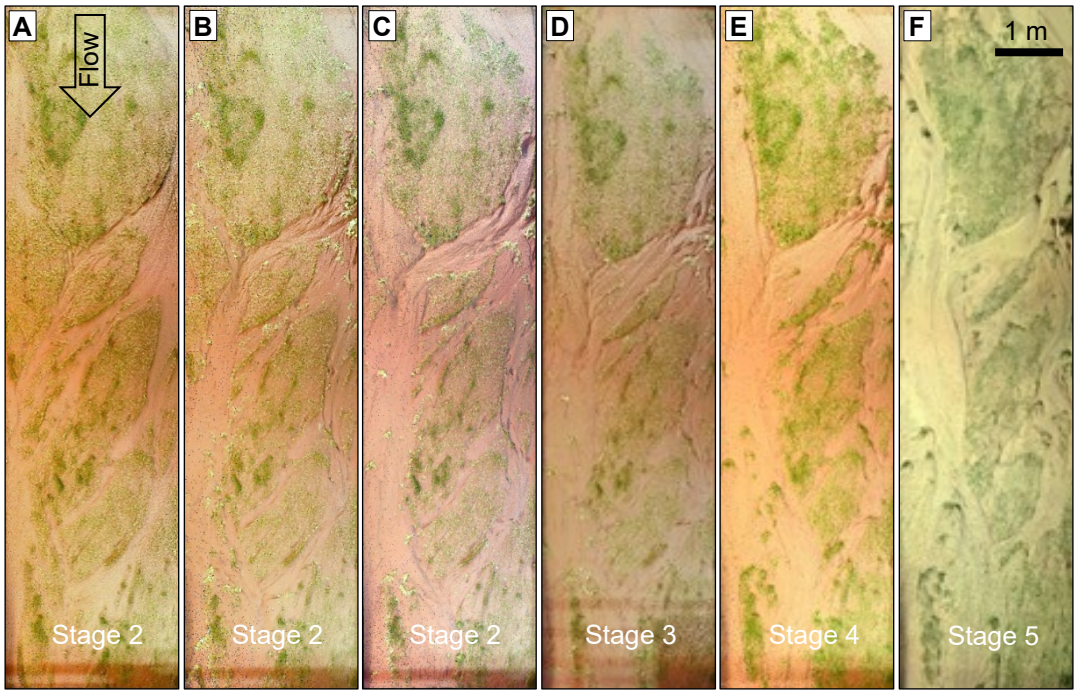

Figure 3 Vegetation cover during the sequence of floods in Flume 1: **a)** plants with 8 days of growing: river bed at the beginning of Run 5 (i.e., Stage 2); **b)** plants with 8 days of growing at the end of Run 5 (Stage 2); **c)** plants with 8 days of growing at the end of Run 7 (Stage 2); **d)** 14 days of growing at the end of Run 9 (Stage 3); **e)** 20 days of growing at the end of Run 13 (Stage 4); and **f)** dried stage of the vegetation at the end of Run 16 (Stage 5). Vegetation colonisation was not included in the experiments, and the minor changes in vegetation cover were because of the removal of existing plants by erosion during the flood events.

2.2 | Braidplain topography and vegetation cover data processing

Width, depth and number of channels were computed from the DEM data at equally spaced cross-sections (0.20 m) along the 8 m study river reach (see Figure 4a). This process was done after filtering the vegetation cover in CloudCompare software (Version 2.10.alpha) by using the CANUPO plugins (Brodu and Lague,

2012). For each cross-section the averaged bed elevation value was used as threshold to discriminate between bars and channels (see Figure 4b). The width-depth curve *b*(*D*) was obtained by integrating depth from zero to the highest elevation in each of the cross-sections, and then summed for the entire 8 m study river reach following the method described in Redolfi *et al.* (2016), $b(D) = 1/L \int_0^L b_x(D)dx$, where *b* is the width of the section for a projected water surface located at a distance *D* (being *D* the distance measured with respect to the lowest elevation obtained on the given section, see schematic Figure 4b). *L* is the reach length (8 m) and *x* is the longitudinal coordinate. The approximation of the curves as a power law, $b = kD^{\propto}$, where the constant *k* defines the scale of the width (Redolfi *et al.,* 2016), was applied here for vegetated conditions to determinate the impact of the plants on the development of the channel width-depth ratios during the sequence of floods. In this regard, the shape of the cross section and channel pattern were identified by looking at the value of the exponent α, as α < 1 indicates single-thread rivers with classic concave upward shape, and α > 1 typifies a concave downward shape associated with braiding river patterns (see Toffolon & Crosato, 2007; Redolfi *et al.,* 2016).

To quantify the relative mobility of the channels during the sequence of floods, the temporal and spatial topography dynamics of all available cross-sections located every 0.20 m within the 8 m river reach were considered. A bed topography correlation coefficient (r_0) at each cross-section between sequential post-flood profiles was computed based on the methodology proposed in Gran & Paola (2001):

$$r_0 = \frac{\mathrm{cov}(\eta_1,\eta_2)}{\sqrt{\mathrm{var}(\eta_1)\mathrm{var}(\eta_2)}} \quad (1)$$

where η_1, η_2 are the sequential cross-section data measured between 1 hour flood event. A value r_0 = 1 denotes exact correlation between the successive cross-section forms, while lower r_0 values indicate higher channel mobility rates.

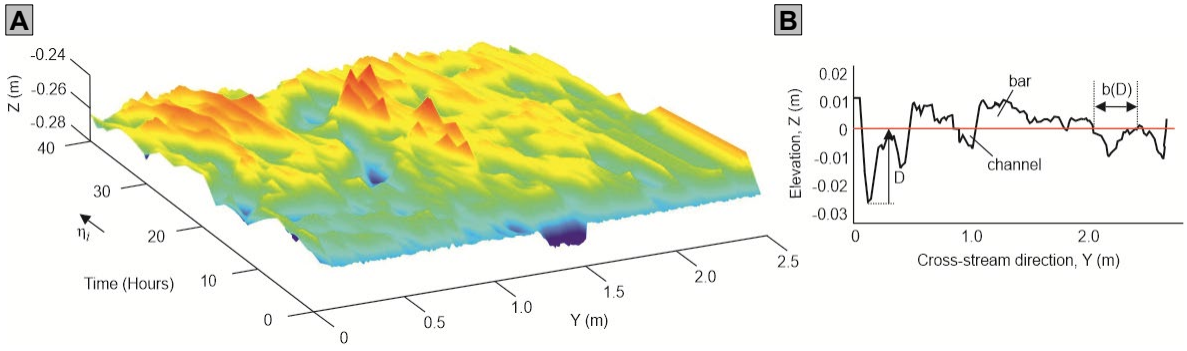

Figure 4 a) Temporal evolution of one exemplifying cross-section; for *t* = 0 the bed-elevation corresponds to the rectangular channel carved by the scraper. **b)** Cross-sectional averaged bed elevation (red line) used to discriminate between bars and channels. Also, example of any width b(D) as a function of the elevation D with respect to the lowest point.

To quantify the impact of vegetation on the number of channels (i.e. braiding intensity, BI) during the low and high floods, the variable ΔBI, relative to the unvegetated conditions, was computed from

$$\Delta \mathrm{BI} = \frac{<(\mathrm{BI_{LOW}} - \mathrm{BI_{HIGH}})^2>}{<(\Delta \mathrm{BI_0})^2>} \quad (2)$$

where the brackets denote an arithmetic mean, i.e., averaged over the analysed 8 m length of the flume channels, and ΔBI_0 is the averaged difference in braiding intensity between high-low flows computed for the sequence of floods in unvegetated conditions.

To track the total vegetation cover, the area covered by plants was identified using color images superimposed on DEMs collected after each flood event. For each image, the number of pixels that were identified as green relative to the total number of pixels along the reach length of the river was calculated. An example of the colour data associated with each DEM data is shown in Figures 5a and 5b for Run 5 (in Flume 1). Using the estimated values of vegetation cover following each flood event, Figure 5c shows the evolution of the vegetation quantified for each growth stage (Runs 1-14). As it is shown in Figure 5c, vegetation cover was close to zero value after Run 4, so a reseeding was done before continuing with the experiments. Only one reseeding was completed in the whole experiment, and in this instance, the alfalfa was allowed to grow 8 days (instead of 4 days) before the release of the flood events. Eight days of growth ensured that vegetation was not easily uprooted (as indicated by the values of vegetation cover in Figure 5c) and the plants that were not removed in Stage 2 continued to grow increasing their chances of surviving the following floods. Therefore, as expected, the removal rates were low in the following stages. Based on the growing root depths shown in Figure 2b, it is evident that the alfalfa remained stable over time after reaching a threshold length of ~0.03 m, and because of that, vegetation cover remained at about 40% of the total area during Stages 2-4 (Figure 5c).

To the end of the experiment, in Stage 5, the vegetation was exposed to drought conditions and weedkiller (about 6 liters of Weedol spray) with the intention to weak and dry out the plants, as it is illustrated in Figure 2c. These dying conditions for the vegetation facilitated the removal of the plants in a similar way than with the young vegetation in Stage 1, as suggested by deduction in coverage shown in Figure 5c after day 15.

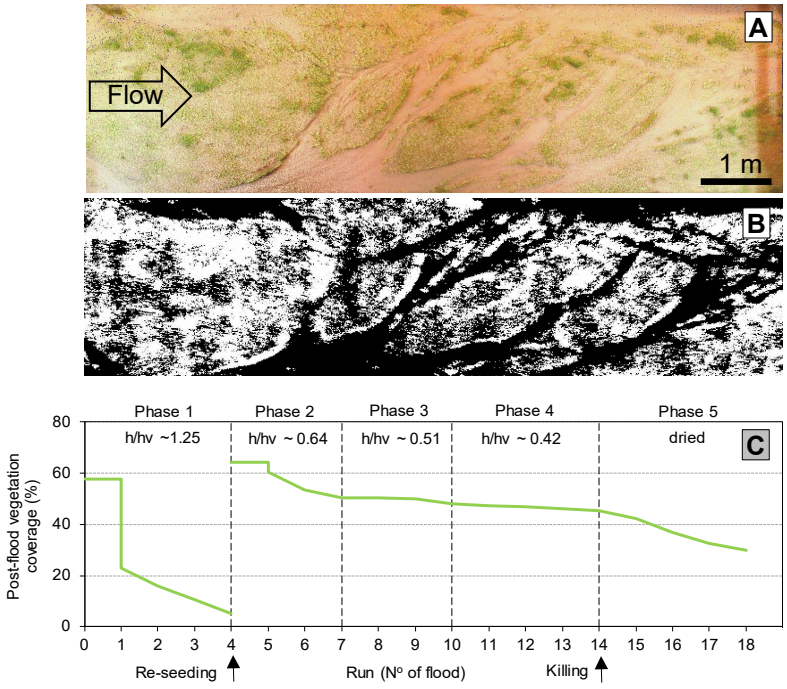

Figure 5 Performance of riparian vegetation coverage during *Experiment II*. **a)** An example of a colour digital elevation map in which vegetation covers about 60% of the total river area (Flume 1, before Run 5). **b)** Binary diagram of the vegetation distribution after extracting the green channel from the image a) utilised to calculate vegetation cover. **c)** Riparian vegetation area as a fraction of total area during the sequence of floods. After Run 4 there was not plant left (<5% of the total area) so a reseeding was performed to continue with the following runs.

2.3 | Up-scaling

By considering a 1:100 generic scale, the experimental setting described herein can be well though as a hydraulic, Froude-scaled model of a non-specific braided stream prototype with a reach length of 1000 m and mean width of 250 m, subject to a sequence of floods with discharges of 200 m^3/s and 300 m^3/s or return periods of 2 and 5 years. A number of rivers can be found in nature with the characteristics of this prototype scale. For example, the upper Drôme River in France has a width ~110 m, d_{50} ~30-50 mm, and discharges of 256 m^3/s and 381 m^3/s with 2 and 10 years return period, respectively (Landon *et al*., 1998). With a similar slope to the one chose in the present experimental setting it is found the gravel-bed Tagliamento river in the Northeast of Italy, which in the upper island-braided floodplain reach presents a slope of ~1.65%, widths in the range of 100-200 m, and where the 2- and 5- year return period floods are estimated to be 1100, and 2150 m^3/s, respectively (Gurnell *et al*., 2000, Arscott et al., 2002). The vegetation used in the present experiments had a stem thickness of 1 mm which would scale up to a 100 mm trunk thickness of a real riparian vegetation, and a height of 30 mm for the vegetation would scale to 3 m in a prototype. For example, trees in Tagliamento river has been reported with these dimensions (Gurnell *et al*., 2001; Gurnell & Petts, 2006).

3 | RESULTS

3.1 | General observations

The observations presented herein focus on the main experiment, *Experiment II*, with growing vegetation. The results from *Experiment I*, which modelled the unvegetated river system, are only presented as a control experiment. Therefore, Figure 6 shows the vegetated river system evolution for the whole *Experiment II* in Flume 1; with each panel displaying the river morphology at the end of each run or flood event.

As described in the methodology, during the flood sequence there was no plant colonisation. The experiment was thus designed to isolate vegetation effects that remained consistent or varied across the simulated vegetation life stages through the sequence of flood events. At the start of the experiment, it was observed that the low-magnitude flood in Run 1 tended to be confined to the pre-existing channels for a short time, after which much of the streamside vegetation began to be removed by the flood water and then the channels started to migrate. As the height of the alfalfa plants increased in subsequent Stages (2,3 and 4), it was observed that flow velocities were slightly reduced, up- and down-stream of plant near the vegetation regions, which caused a rapid acceleration of flow in confined channels and diverted the flow towards less vegetated zones. Some of the released bedload was deposited proximal to vegetation which increased the height of bar-tails, as shown in Figure 6k and 6n; these effects become more pronounced over time as the plant height increased. As the experiment progressed, established vegetation patches were not removed by the flood events (vegetation cover remained mostly constant as shown by Figure 5b), and channelization was slightly increased by flow bifurcation, particularly during the low flow events.

Reach-averaged flow velocities, estimated by releasing dye and particles during the experiments, ranged from 0.20 to 0.40 m/s approximately. The flow Froude number Fr (computed as $U/(gh)^{0.5}$, where U is the average velocity of the flow, g is the acceleration of gravity, and h (~0.02 m) is the flow depth) it was within the range of 0.4-0.9 and increased to unity (and ~1.2) in some confined reaches. Mean wetted widths of cross sections were W ~ 1.6 - 2 m during the flood events, yielding Reynolds numbers Re in the range of 1000 - 2000 (computed as $Q/\nu W$, where ν is the water kinematic viscosity). This indicates the experiments were in the transition to a turbulent regime. The values presented above are similar to that obtained in previous studies of vegetated braided rivers, as the Tal & Paola's experiments (2010), in which Froude numbers were reported in the range of 0.2 - 0.8 and a fully rough and turbulent flow was characterized with Re > 2000.

During the flood events with a sediment deficit, i.e. Runs 3, 13 and 17, in which the bed load supply was reduced to 80%, it was observed that the flows removed much of the sediment storage behind vegetation patches, as illustrated by Figure 6m which shows a post-deficit channel morphology. The flood events that followed these deficit floods were recognized here as 'recovery' flood events, since these flow with equilibrium sediment supply rates reversed the effects of the previous flood events in terms of the morphodynamic changes. In particular, it was observed that following a deficit experimental run, the subsequent flood event tended to differentially fill the scour zones first, and deeper the channels left by the previous flood; hence the longitudinal bed slope of rivers remained almost constant throughout the experiments.

With the vegetation cover remaining roughly constant during the experiments as shown by Figure 5, the present study examined the effect of a flood sequence in a system with a riparian vegetation that remained almost spatially invariable (with a survival rate greater than 90% during Stages 2-4, see Figure 5c), but with plant size increasing due to vegetation growth (as it was shown in Figure 2b). Under these vegetation conditions, the overall planview configuration of the braided rivers also remained mostly unchanged during Stages 2-4, with vegetation and associated bars staying in place, and channels keeping roughly the same paths. With a mean flow depth during flood events of about h~0.02 m measured during the experiments, the different plant stages considered in this study can be associated to a varying relative submergence h/h_V, where h_V is the mean averaged height of the vegetation canopies (as given in Figure 2b). The approximate values for the relative submergence for Stages 1-4 are added in Figure 5c to indicate the modelled vegetation conditions in terms of the above ground part of the plants that were analysed during the experiments; only during Stage 1 the vegetation might be covered by the floods.

Towards the end of *Experiment II*, the decaying vegetation conditions reduced the stabilizing effect of the vegetation and encouraged the formation and development of new channels in those areas previously dominated by living vegetation. Hence, Stage 5 of the experiment was comparable to Stage 1, with both decaying and young vegetation being unable to control the morphodynamics of the rivers. During the entire sequence of floods, a number of distinct morphodynamic processes were identified in association with the effects of vegetation age (size), which is described in greater detail below.

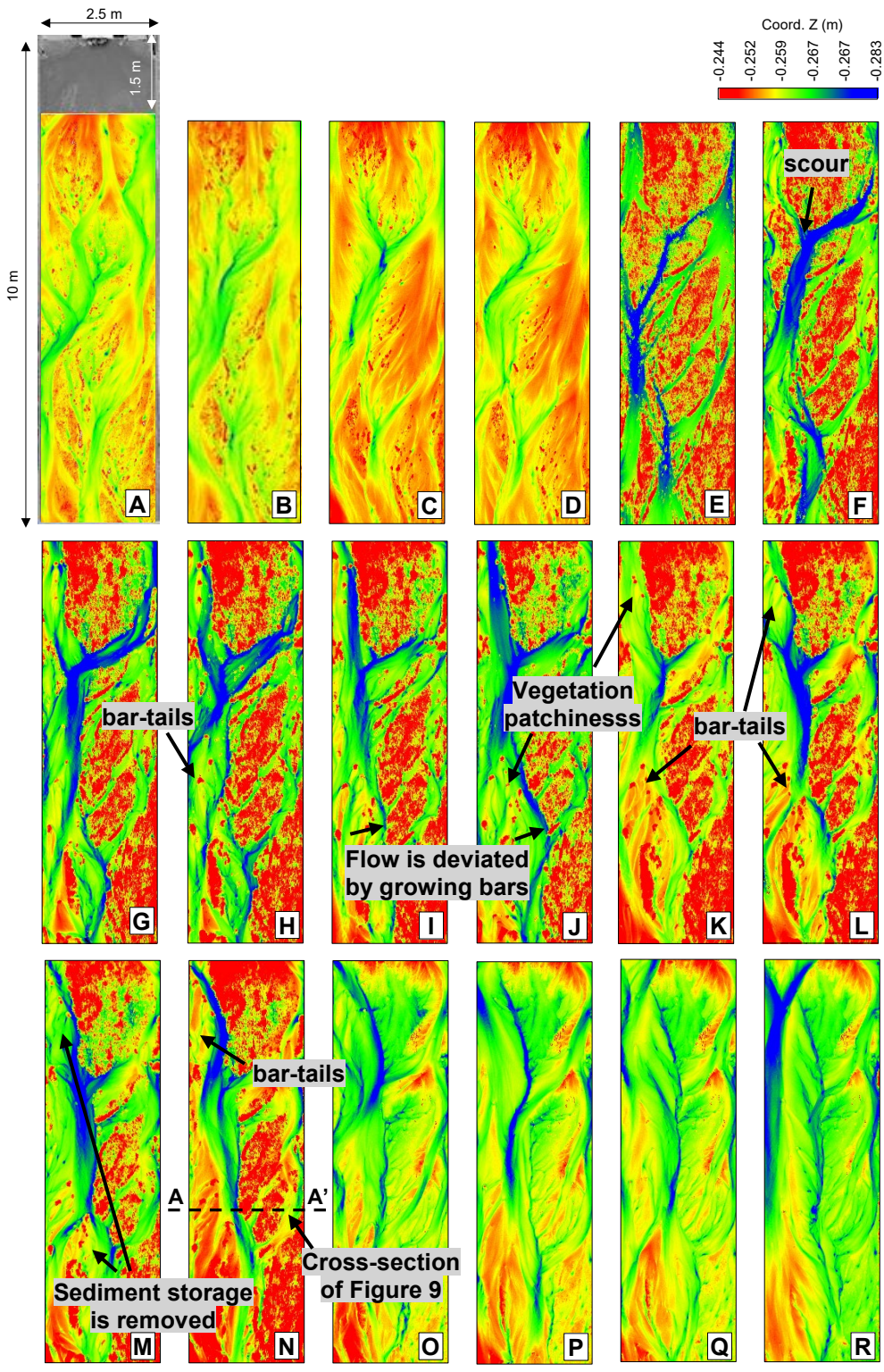

Figure 6 Post-flood morphological changes of the vegetated river bed in Flume 1 measured by laser during *Experiment II*. Each panel shows the braided river pattern at the end of each

hydrograph Run 1-18; Stage 1: A-D, Stage 2: E-G, Stage 3: H-J, Stage 4: K-N, and Stage 5: O-R, Flow direction is from top to bottom. Panels I-J shows the role of sediment bars (particularly, sediment stored behind plants during low floods) in deviating the flow (particularly during high floods). Panel M illustrates the changes of the river bed at the end of Run 13, which had a bed load input reduced, leading to the pronounced removing of the stored sediment. Panels O-R correspond to Stage 5 with a dried braidplain vegetation condition, which caused also a pronounced removing of sediment stored behind plants during previous runs.

3.2 | Topographic adjustments

3.2.1 Erosion and deposition rates

The DEM data was processed to characterize the planimetric dynamics of the rivers during the sequence of flood events (see methods section). The average volumetric deposition rates were measured by differencing the topographic scans collected at the start and at the end of each flood event, summing the difference values at all locations, and dividing by the duration of the event, i.e. one hour. The result was the volumetric rate of deposition (positive) or erosion (negative) at the reach-scale shown in Figure 7 for all the runs that included vegetation, i.e. *Experiment II*. The role of vegetation in increasing aggradation rates and reducing erosion (resulting in positive net values) was verified in most of the runs. Runs 3, 13 and 17 in Flume 1 during *Experiment II* were with a sediment deficit within the inflow and as expected, the net values were negative showing increased erosion. In all cases, the flood event that followed a deficit flood differentially filled the deeper channels left by the previous flood event. In particular, it was observed that during all the stages of alfalfa growth (Stages 2-4) the erosion rates were lower in both flumes, and they only started to increase during Stage 5 when the vegetation

was desiccated. Note that net values were negatives during Stage 5 of the experiment, because the flood events removed most of the sediment that was stored in the lee of vegetation.

3.2.2 Area of topographic change

Figure 7 shows that the proportion of topographic change decreased from 40% and 50% during the low and high flood events, respectively, to about 30% of the total river area by Run 6, and remained constant in this value thereafter during Stages 3 and 4 (*Experiment II*). In this respect, the area covered (and therefore stabilized) by vegetation that was observed earlier in Figures 6g to 6n appears to have limited the proportion of area of change during Runs 8-14 (Stages 3 and 4) as established plants could not be removed by the floods. In contrast, results from Runs 15-18 during Stage 5, show that the area of change started to increase when the vegetation was in decline. The percentage of area that changed during the floods in Stage 1 (young vegetation) was comparable to the one computed in Stage 5 (desiccated plants).

Comparing the high and low flood impacts on the topography, the areas of topographic change typically increased for the high flood events in about 10%, which might be linked to the increase in the area of exposed bed to the flood. In this regard, DEM data measured during the floods showed that during high-magnitude flood events, the water flow covered an area approximately 15% larger than that during low-magnitude flood events, and this difference is reflected in the area of topographic change calculated during the experiments.

Regarding the sediment being flushed from the river out of the system during the succession of floods, this reached the lowest value during Stage 3. This is shown in Figure 8, in which the sediment transport efficiency was computed as the ratio between Q_{out} (sediment weighed at the downstream end of both flumes after subtracting the water content) and Q_{in} (dry sediment fed into both flumes). During the succession of runs, it is evident from Figure 8 that vegetation limited sediment transport towards the downstream end of both flume channels, enhancing aggradation along the river reaches. Part of this retained sediment was stored behind vegetation leading to bar-tail formation on the right side of the river, as it is shown in Figures 6g-6n. The results in Figure 8 clearly show that even though vegetation density remained comparable during the sequence of runs (as vegetation colonisation was not included in the experiments) the sediment transport efficiency varied during the different life stages of the established vegetation, and it attained the reach-averaged minimum value of 48% in Stage 3 (in both flumes). Further, Figure 8 illustrates the bedload transport efficiency for Runs 3, 13 and 17 (in Flume 1) that were the runs with a low-bedload input. Clearly, these deficit runs were effective in removing sediment along the river length and increasing the delivery of sediment at the downstream end of the flume, with computed values of the ratio Q_{out}/Q_{in} ~ 3.5, 2.2 and 5.2, respectively. In addition, it was noted that the highest value of sediment being delivered by the river happened to the end of the experiment during the drought conditions, i.e. in Stage 5. Therefore, with the above-ground of the biomass being dried, floods were able to remove most of the sediment stored during previous floods.

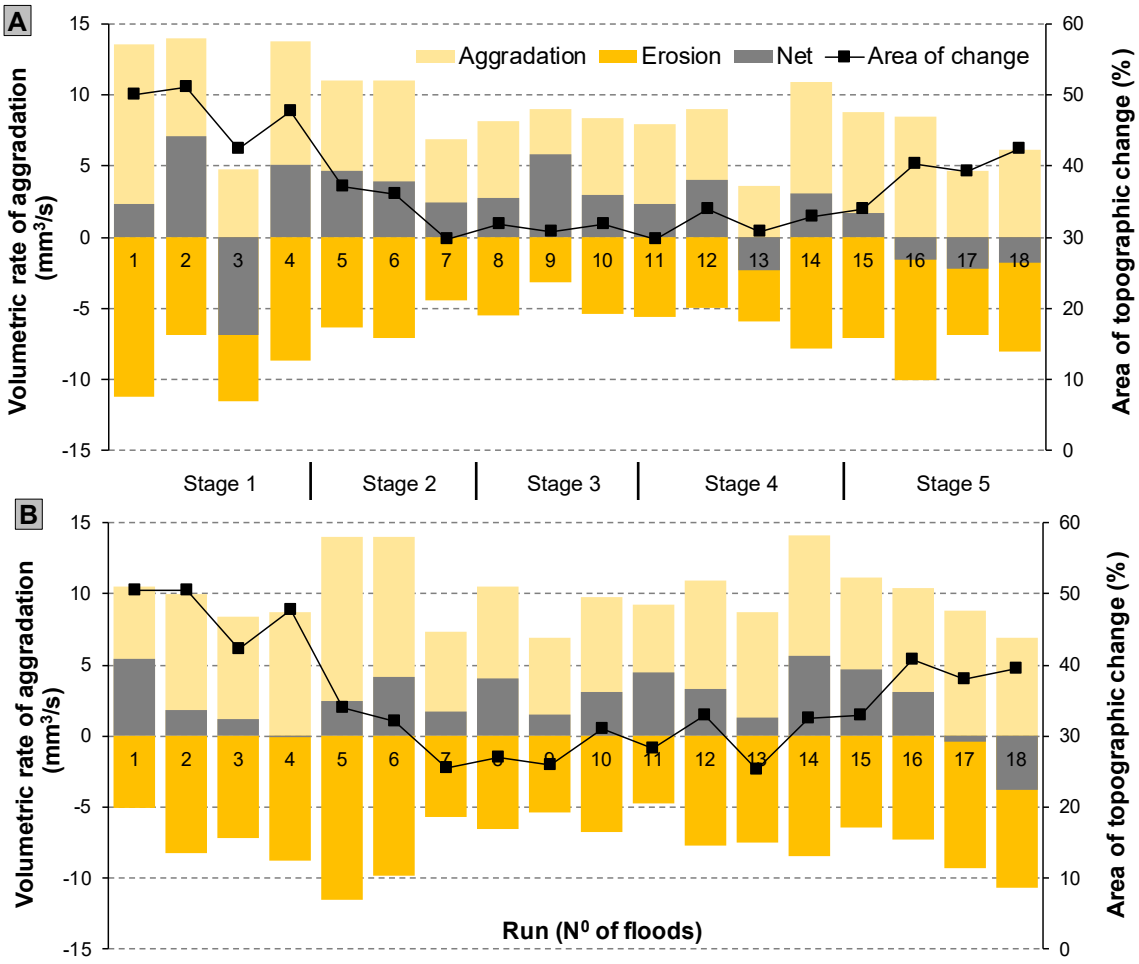

Figure 7 Post-flood changes in the total volume of erosion, aggradation and net topographical change within the river reach over the sequence of the 18 runs in *Experiment II* in: **a)** Flume 1; **b)** Flume 2. The area of topographical change is also shown. Runs 3, 13 and 17 in Flume 1 were with deficit in sediment within the supply, therefore the net values are negative for those runs.

3.2.3 Local scour

The maximum depth of bed scour was extracted from DEM data and contrasted with the maximum depths measured during *Experiment I* with no vegetation. The averaged bed elevation value in each DEM was used as reference to compute the maximum depths that are shown in Figure 9, together with the reach-averaged

mean depth of the channels to give an indication of the overall channel depth distribution. This demonstrates that the presence of vegetation in *Experiment II* increased the channel scour depths relative to the unvegetated scenario of *Experiment I*. Indeed, the depths of the scour zones for unvegetated channels were about 1.5 times the mean depth of the channels, and increased to 2.5 times with mature vegetation. Overall, the maximum scour depths were within the range of typical values of 2-3 times the depth of the tributary channels measured in previous experiments and field studies (e.g. Mosley, 1976; Ashmore & Parker, 1983; Best, 1986), but for the established vegetation in Stage 4 the maximum scour depths were the largest.

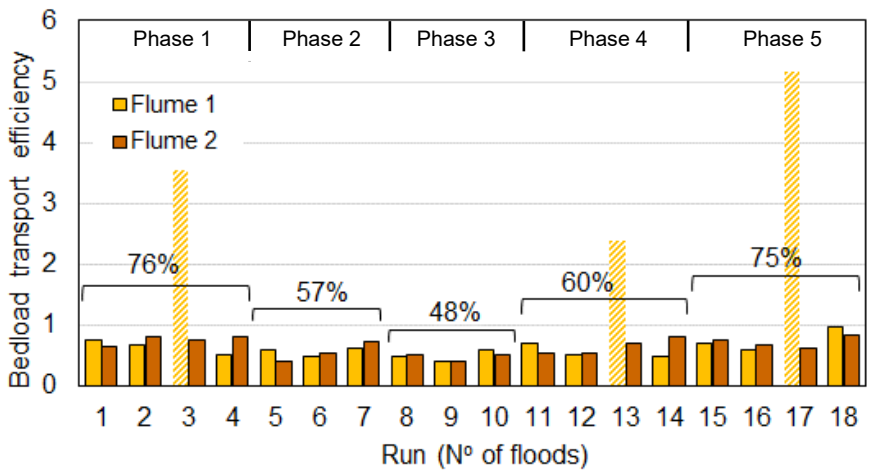

Figure 8 Bedload transport efficiency computed as the ratio Q_{out}/Q_{in}. The vegetation life stages played a major role in controlling the impact of the sediment delivered by the rivers. The three pattern filled bars indicate the three runs with deficit in sediment introduced in Flume 1. The percentages are the averaged value of the transport efficiency ratio in both flumes without considering the sediment deficit runs.

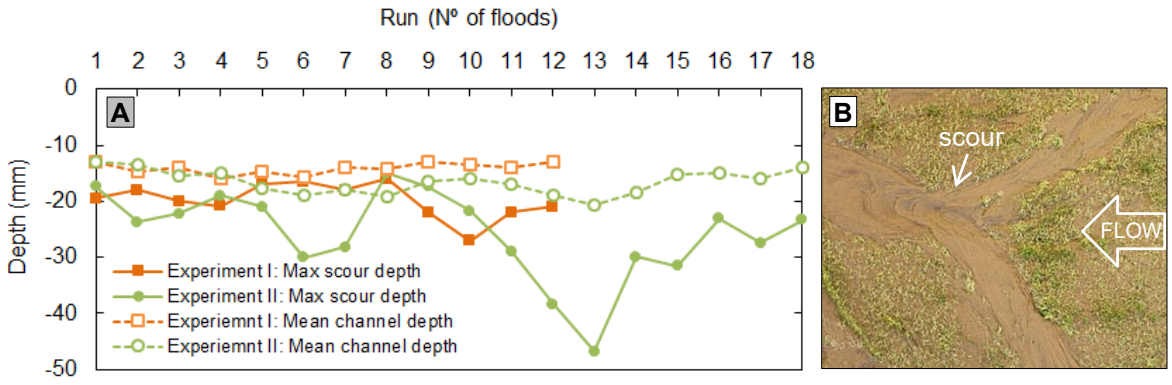

Figure 9 a) Maximum scour depths and reach-averaged channel depths measured during the release of flood sequence in Flume 1 for bare (*Experiment I*) and vegetated bed conditions (*Experiment II*). **b)** View of a typical scour formed at a confluence morphology after Run 5 indicated in Figure 6e.

3.3 | Channel dynamics

At the locations with vegetation, and with vegetation growth, the river bed (and the channels) was stabilized by the plants but the system remained highly dynamic with migrating channels in any area without vegetation, or with sparse vegetation with patches smaller than ~0.07 m diameter. This is shown in Figure 10 which illustrates the evolution of a cross-section located 6 m from the inlet during different stages of *Experiment II*. Contrasting with Stage 1 (young vegetation) and Stage 5 (decaying vegetation) illustrated in Figures 10a and 10c, respectively, Figure 10b clearly shows the lack of mobility of the bed where vegetation existed during Stages 3 and 4.

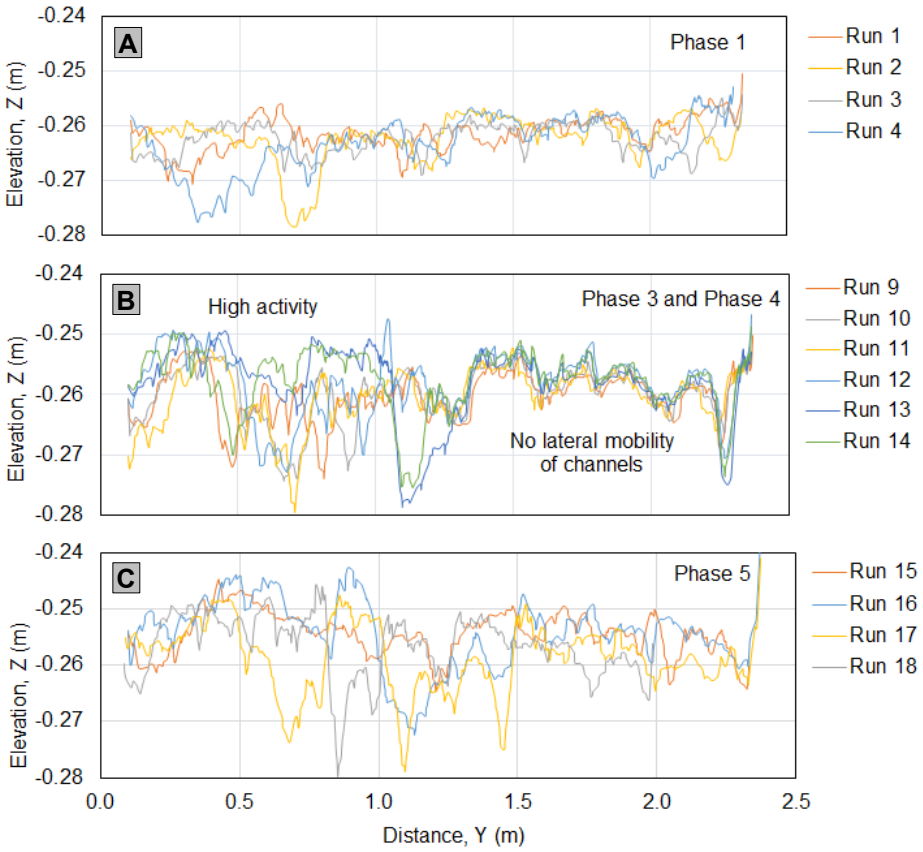

Figure 10 Examples of cross-section changes at 6 m from the upstream boundary in Flume 1 in: **a)** Stage 1 with young vegetation, **b)** Stages 3 and 4 with established vegetation; and **c)** Stage 5 with dried vegetation. Flow direction point to the observer.

To quantify the relative mobility of the channels, the topography correlation coefficient (r_0) at each cross section between sequential profiles was applied based on the method described in Gran & Paola (2001). Figure 11 indicates that the coefficient r_0 varied between < 0.1 to 0.8 for individual sections. The reach-averaged values of the coefficient (along the 8 m river length analysed) were around 0.25 during Stage 1 and increased to about 0.45 during Stages 3 and 4. In

contrast, during Stage 5 (i.e., dried vegetation) and also during unvegetated conditions (*Experiment I*) the coefficient was about 0.2.

As the vegetation grew, flood events (particularly the low-magnitude events) were not able to remove vegetation patches formed earlier in the rivers (see Figure 6j-6k), and this patchiness contributed partly to channelization by bifurcating the flow. To quantify how bifurcations and braiding developed in the river systems, the braiding intensity (BI) was measured by calculating the number of channels during the sequence of floods. Figure 12a shows that the presence of vegetation in *Experiment II* increased the total number of channels by two, relative to the unvegetated conditions (*Experiment I*).

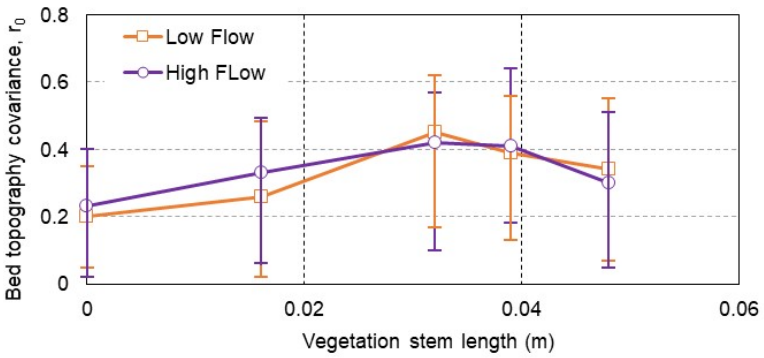

Figure 11 Impact of vegetation growth on the reach-averaged bed topography correlation coefficients for the low and high flood magnitude events. The calculated mean and max-min values of the variation of r_0 are also shown in the figure. Following Figure 2b the root length of the plants could be alternatively used to the vegetation stems.

It is worth of note also that the no vegetation condition (*Experiment I*) leaded to an increase of the reach-averaged BI in about +2 channel during the low flood

events relatively to the high flows (Figure 12a). This influence of the flood magnitude on the number of channels was less evident in presence of vegetation. To quantify the impact of vegetation on the BI differences between the low and high floods, the variable ΔBI was computed relative to the unvegetated conditions (i.e. *Experiment I*, with ΔBI_0 = 1.2 in equation 2).Figure 12b illustrates that ΔBI was less sensitive to the flood magnitude (or to flow variability) during Stages 3 and 4 (14 and 20 days of growing). To characterize the variability of BI for the different flows, the probability density functions (pdf) of the BI during Stages 1 and 5 (which presented the highest relative mobility rates of channels as shown in Figure 11) is reported in Figure 12c. The pdfs exhibit a distinct peak at BI = 6-7 for the case of the low flow events and BI = 5-6 for the high flows. In addition, it should be noted that the profiles are narrower in the case of the high flow events, and the number of channels most likely to be observed is in the range ±3 from the mean value, while for the low flows this is in the range of ±4.

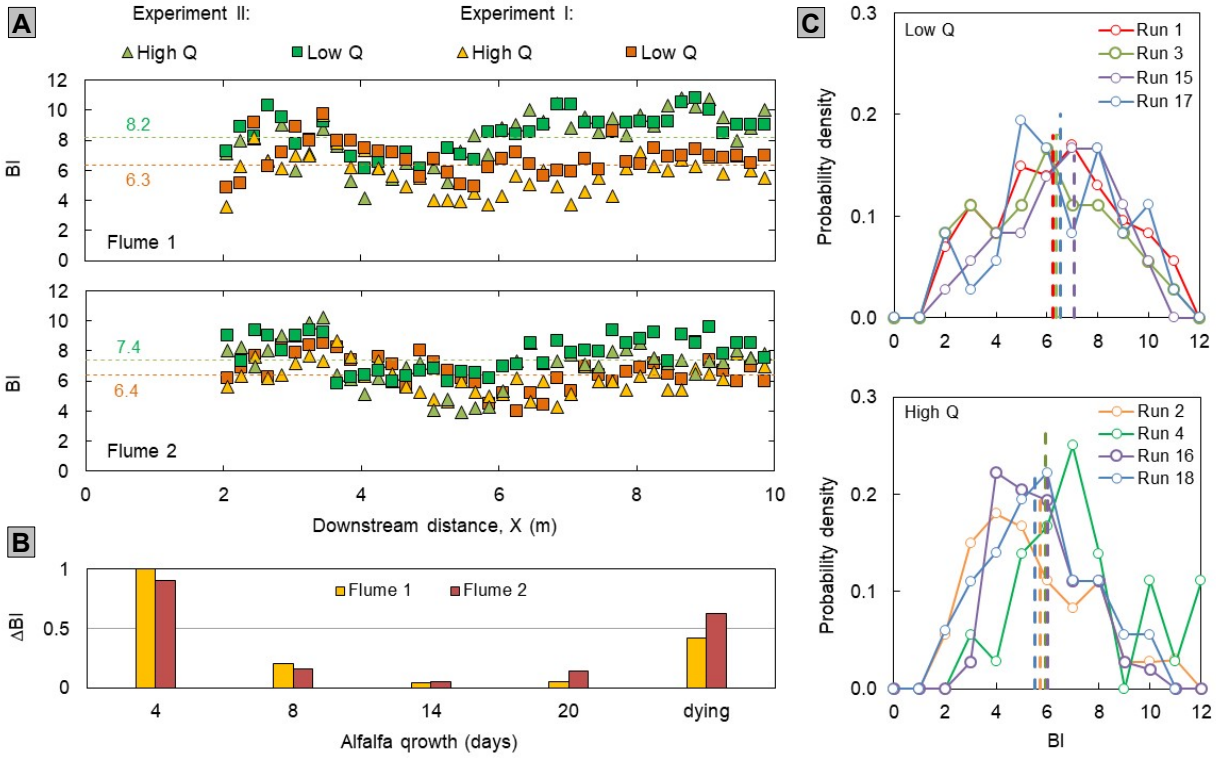

Figure 12 Braiding intensity. **a)** Averaged BI values for all the runs performed with no vegetation (*Experiment I*) and with vegetation (*Experiment II*). The dashed lines indicate the mean value for both flows computed along the analysed river length. **b)** Relative differences of the braiding intensity between high and low floods as computed by expression (2) for the different vegetation life stages (stages) of the experiments; and **c)** Pdfs of the number of channels for low and high flows. The dashed vertical lines are the mean BI values averaged over the 8 m study flume length.

3.4 | Width/depth ratio and bar height

The growth of vegetation during the experiments tended to erode the channels and also to increase the spatially average elevation of the bar surfaces, as shown in Figures 13a and 13b. These figures clearly show that the topographic response was sensitive to the characteristic length of the plants (i.e., root and stem mean lengths). In particular, the taller plants of Stages 3-5 can be linked to greater aggradation relative to the condition with no vegetation (i.e., the condition for L_{root} = L_{stem} = 0 in Figure 13).

Regarding the influence of the root depths, (and based also on the previous Figure 2b that shows the growth curve for the roots), Figure 13b indicates that Stage 1 (Runs 1-4) reported channels depths deeper (~0.014 m) than the plant rooting depth (~0.005 m, Figure 2b), so that plants could be removed by bank undercutting. Stages 2-4 (Runs 5-14) were floods with plant roots (~0.03 - 0.043 m) that were deeper than the channel depth (~0.015 - 0.021 m), which limited vegetation removal during those stages of the experiment.

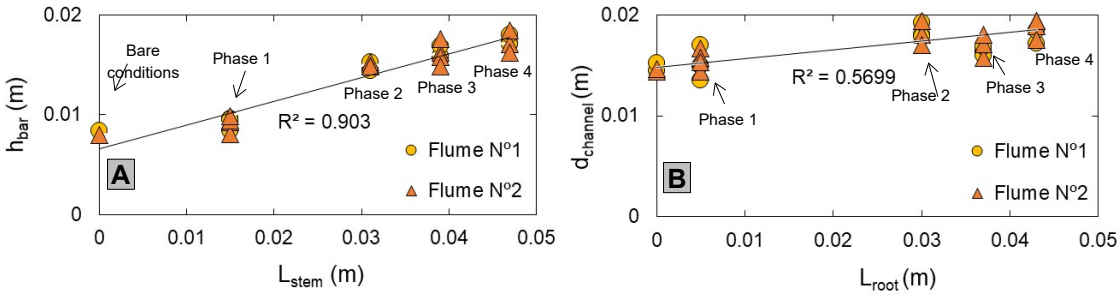

Figure 13 Maximum geometric values spatially averaged along the river reach against the characteristic plant lengths, for bare conditions (L_{root} = L_{stem} = 0) and during growing vegetation (Stages 1-4). **a)** Bar height against stem length; **b)** Channel depth against root length.

Figure 14 shows all the reach averaged width-depth curves calculated for the sequence of flood events in Flume 1 during each of the five vegetation growth stages considered in this study. The agreement between the power law and the computed $b(D)$ curves was in general strong in this study, since the determination coefficient, R^2, was typically larger than 0.93 in all the studied cases, as it is shown in Figure 15a. Figure 15 also illustrates that the calculated values of the coefficient α increased from 1.3 in unvegetated conditions to 1.5 with the addition of vegetation, demonstrating that the presence of vegetation increased the topographic variability of the braiding rivers.

Regarding the impact of the flood magnitude on the topography, Figure 15 indicates that the low-magnitude floods tended to increase the values of the topographic variability measured here by the exponent α relative to the high-magnitude floods, with a mean value that increased from α = 1.43 to α = 1.49. The difference in between high and low floods was observed to be minimum in Stage 3

(in which the alfalfa was 14 days old); for those runs the values of coefficient α was 1.49 and 1.50 for the high and low magnitude floods, respectively.

The sediment deficit within the supply in two of the low floods, it was observed to reduce the value of the coefficient to α = 1.44 (see Figure 15), so that, diminishing the impact of vegetation and making those runs to perform comparably to a high-magnitude flood event. It is worth noting that Figure 15 summarises the impact of both vegetation and flood-magnitude on the morphology. Low-magnitude floods lightly increased topographic variability relative to the high-magnitude floods, and vegetation also increased it relative to bare conditions, but this impact varied based on the vegetation life stage.

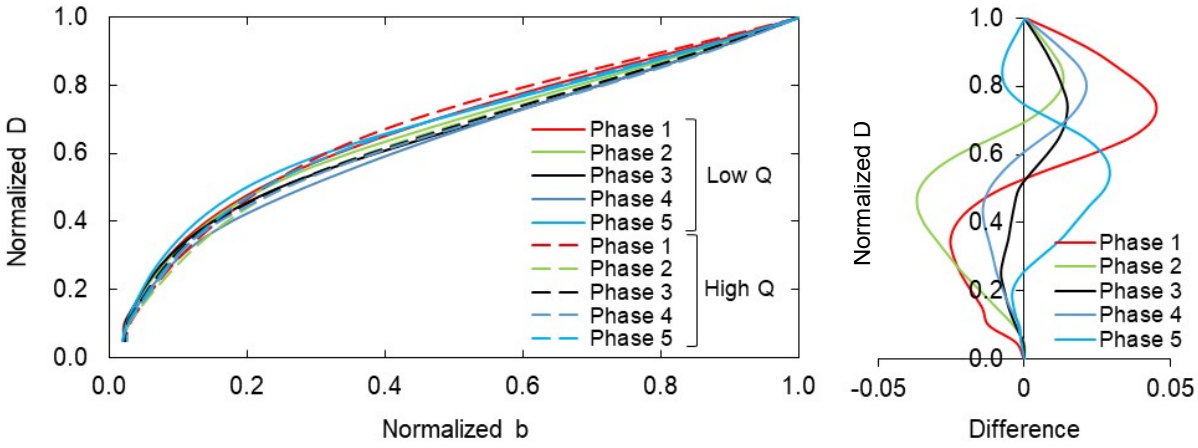

Figure 14 a) Normalized reach-averaged width-depth curves in Flume 1 for *Experiment II*. **b)** Computed difference between the high and low flood curves illustrated in a) for each Stage.

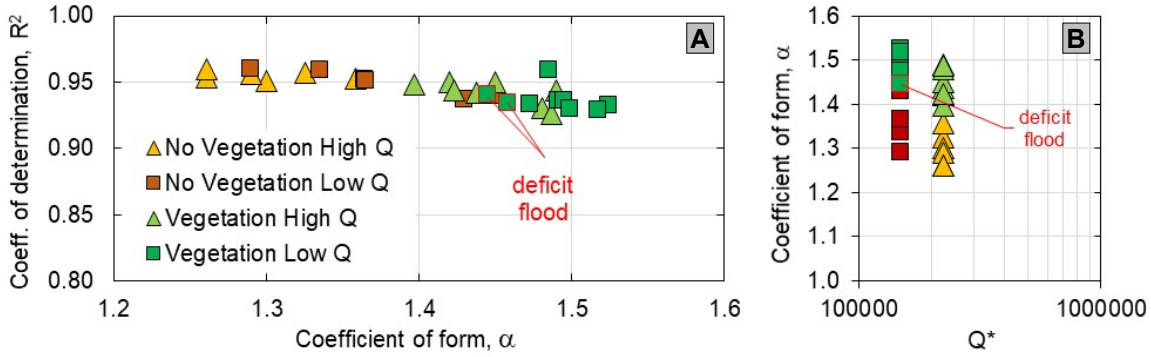

Figure 15 a) Coefficient of determination (R^2) against coefficient of form (α) from the power law approximation to the width-depth curves shown in Figure 14a (*Experiment II*), together with the computed values for the runs with no vegetation (*Experiment I*). Clearly, the addition of vegetation increased the value of α, so that, the degree of bed irregularity. The sediment deficit in the floods indicated in red reduced the value of α in relation to the small equilibrium floods, making those small floods to perform comparably to the high flood events. **b)** Coefficient α against the scaled small and high flood discharge Q^*. The trend of the coefficient α to increase for the runs with vegetation (in both low and high magnitude floods), suggests the decline of channel confinement by vegetation relatively to the condition with no vegetation.

4 | Discussion

4.1 | Experimental limitations and the role of plant colonisation in the river pattern

The present experiments confirmed sequential changes to river morphology driven by flow variability over five different vegetation life stages. Arguably the most interesting result shows that the absence of plant colonisation leads to an increase in the numbers of channels. In this context, the present work can be contrasted to Tal & Paola's experiments (2010) in which their rivers transitioned from braided to

a single-thread channel. Tal & Paola's experiments were conducted in a flume 16 m long and 2 m wide, with a bed slope and Froude and Reynolds numbers in the same range than the present experiments. However, by allowing vegetation colonisation (or pre-flooding seeding) during the cycle of seeding-growth-flooding-seeding, the riparian plants played a major role in reducing the number of channels which contrasts with the present results. In Tal & Paola's experiments flood frequency seemed not to be relevant on the trends of river morphology, and the impact of flow variability was not addressed by the authors. In nature, however, flood frequency still might impact the young vegetation and colonisation between flood events might not take place, as it was reported in Gurnell & Petts, (2006) and Crouzy *et al*. (2012). The present results address this condition: the impact on braided morphologies due to flow variability in situations where colonisation might be restricted by different factors like vegetation removal, prolonged droughts or inundation above the plant's tolerance. Following the up-scaling denoted in section 2.3, the floods that were investigated in this study did not model extreme events, but were focused on events with return periods of 2-5 years that may be related to the absence of plant colonisation due to the frequency of the floods.

A better understanding of the impact of short-term flow variability on channel-vegetation interactions is necessary in modelling studies to evaluate the effect of temporal ordering of frequent hydrologic events, which would control river systems on timescales up to decades in length. In this regard, Baynes *et al*. (2018) highlighted that timescales of years to decades are critical to understand climate change impacts on riverine systems and managing adaptation to climate change. At these timescales, and without any significant anthropogenic impacts, the

average bed profile of natural rivers is likely to be in quasi equilibrium, i.e. the mean elevation of the active bed does not experience significant temporal variations (e.g. Pittaluga *et al*., 2014). In this respect, the experimental setting described in this work refers to this situation, as the sediment loads for the inflows were initially calibrated to keep the initial bed slope of 0.015 m/m constant throughout the experiments. Therefore, with the experiments designed to have the river bed slope set to a constant slope during bared bed conditions, the morphological changes due to flood sequence were constrained to the channel-geometry variations and their interaction with the riparian vegetation.

Five different vegetation scenarios (stages) were studied based on the different life phases (and strength) of the vegetation allowed in the experiments. The young, pioneer vegetation in Stage 1 characterized a high stem density (~1 seed/cm^2) and a network of dense, short roots. During this stage, the impacts of flood sequence on the number of channels compared well with the observations on bared bed conditions of *Experiment I*. Therefore, this stage was geomorphological, with the young vegetation unable to take control on the morphology and highly exposed to erosion processes as suggested by the erosion volumes in Figure 7. Hence, by the end of this first stage, all vegetation cover had been removed by the floods (Figure 5). Also, bedload sediment transport reached a maximum value during Stage 1 (Figure 8). During Stages 2-4, the influence of the vegetation cover on the morphology increased from minimum to maximum, this clearly revealed by the decrease of cross-section changes (Figure 10) and mobility of channels (Figure 11), until vegetation started to die back in Stage 5 to simulate drought conditions. During this last stage, the rivers showed a trend to behave similarly than in Stage

1, particularly with same amount of bedload delivered by the rivers (Figure 8) and comparable bed irregularity (Figure 4).

All sediment in these experiments was transported as bed load and results should be applicable in rivers where suspended sediment is negligible. Also, results presented here are for rivers with a slope of 1.5%. Millar (2000) suggests that such rivers are likely to remain braided, irrespective of the riparian vegetation. Indeed, based on the diagram derived from the model proposed by Millar (2000), for the diameter of the bed sediment (0.45 mm) and flow rates (2-3 L/s) used in the present experiments, a change in the pattern due to vegetation colonisation is only likely for gradients less than 1%. The trend of the number of channels to increase in presence of vegetation observed in the present study not necessarily reflects the impact of the high bed gradient. In this regard, the experiments carried out by Tal & Paola (2010) used an initial slope of 1.5% (and similar sediment diameter and flow magnitudes than the present study), and the authors reported in their experiments that vegetation colonisation discouraged the coexistence of multiple channels even the bed slope was 1.5%. As mentioned above, the present results differ from the Tal & Paola's experiments (2010) which allowed vegetation colonisation (T_{veg} / T_{flood} < 1) and the number of channels decreased as the river evolved into a single-thread system. This study that modelled the opposite case (T_{veg} / T_{flood} > 1) finds more likely support in the experiments from Coulthard (2005), who planted isolated and large, mature plants (vegetation colonisation was not considered) to split the flow and increase the braid index. Flow diversion will encourage the development of new channels and topographic irregularity, particularly during low floods, as in

these events plant submergence was relatively smaller in the present experiments and plants acting as an obstruction trended to increase.

Hence, the transition from a braided to a single-thread channel seems to be intrinsically linked to the dynamics nature of plant colonisation that might occur then when $T_{veg} / T_{flood} < 1$ (i.e. lack of disturbance for the vegetation). But even in periods during which no floods may occur, riparian plants could be sensitive to drought and depth to water table, affecting this availability of moisture on the surface and so that, the colonisation by vegetation. This condition has been reported in the Tagliamento river (Gurnell *et al*., 2001). The river slope of 1.5% used here and in the Tal & Paola's experiments (2010) did not modified the capacity of the colonisation condition (present or absent) to influence the river pattern, and in both experiments was evident the stabilizing role of vegetation. Lastly, although the approach used in this study to compute channels differs from the methodology used in Tal & Paola (2010, i.e. dye release and direct observation), the trend of the river to increase the number of channels instead to evolve to a single-tread river was by far observable.

4.2 | Effects of fluctuating discharge and plant life cycle

For the bare condition of *Experiment I,* the river braiding adjusted to the variable discharge by alternating the number of channels in about ±2. With the addition of the plants (*Experiment II*), results showed that braiding increased, but the susceptibility of the channels to flood magnitude varied with the growth stage of the alfalfa.

During Stage 1, typified by the initial plant life stage (and with root depths that were substantially less than the channel depths), the number of channels fluctuated (in ±2) between defined values established by the magnitude of the flood flows. Following Corenblit et al.'s biogeomorphic succession concept (2007), this first stage can be characterised as the geomorphological stage in which the pioneer vegetation is still unable to influence the river pattern. Then, as the plants grew larger (i.e., Stages 2-4), the effect of flow variability on river pattern was less perceptible as the vegetation was capable of stabilizing the river banks, reducing the rate of mobility of the channels in those areas covered by vegetation (Figures 10 and 11). In these stages of the experiment that can be characterized as the bio-geomorphological stages, the influence of the plants on the morphology increased from minimum to maximum as the vegetation grew older from Stage 2 to Stage 4. Additionally, by likening Figures 8 and 11 it was observed that limitations in channel mobility due to the increased plant strength reached the maximum value in Stage 3 (with a bed topography covariance of about 0.4), in agreement with the lower amount of sediment being delivered by the system. In this context, as reach-averaged aggradation rates remained nearly constant during the experiments (see Figure 7), it is suggested that the varying bedload transport shown in Figure 8 was controlled by the role of vegetation in stabilizing the morphology and in inhibiting the migration of channels, and not just by the role of the plants in enhancing sedimentation. In this regard, as the above-ground biomass is linked to a decrease of flow velocities and channel migration, it is difficult to infer if the above- or below-ground biomass played a more significant role in the delivery of the sediment at the reach scale in the experiments.

In particular, it has been show that after adding vegetation the channel depths slightly increased during the experiment (Figure 13b), and that the root lengths being deeper than channel depths (Stages 2-4) resulted in minimum mobility of the channels (Figure 11). However, In the field, particularly in moister environments, roots may be denser near the surface without a need to access to deep water tables (Holloway *et al*., 2017), what may result in a decrease of stabilization by vegetation.

During the Stage 4 of the experiments, the area covered by the vegetation remained similar to the previous stage (~50% of the total river area); however, the sediment delivered by the system slightly increased (~12%) in comparison to the previous Stage 3. As the local scour depths along the rivers attained maximum values in Stage 4, with holes ~2 times of the depths computed in the previous stage, it is suggested that the source of the increment of the sediment delivered at the downstream end of the rivers in Stage 4 was because the scour holes. It is worth of note that this increase in local scour in the later stages may not only be related to vegetation strength. It could also be related to longer term adjustments of the channel to its vegetated condition, regardless of vegetation characteristics (e.g. Hupp & Bornette, 2014).

The present work also point to the importance of the frequency of floods in influencing the successional Corenblit et al.'s biogeomorphic stages. With a high frequency of hydrologic events, the succession may be interrupted by floods maintaining just a young vegetation stage in the river, like Stage 1 in the experiments. As hydrologic disturbances are less frequent, the succession might have the opportunity to proceed beyond the initial stage and persist to old growth

stages (Stages 2-4). Further, the circumstance that in Stage 5 (decaying vegetation) the number of channels and sediment delivered downstream by the rivers were similar than in Stage 1 with the young vegetation, it could be linked to the resetting capacity of decaying vegetation. Colonisation by vegetation is not easily reversible and it could have long-term effects, but the modelling of drought conditions to the end of the experiments illustrated the significant role that decaying vegetation can have in resetting the river pattern (lack of stabilizing effect and with dried plants acting also as obstacles to the flow, facilitating channel development). Further, Stage 5 point to the role that decaying vegetation may have in the re-initialization of the succession, and so that, the influence that arid or humid environments may have in the reversibility of vegetation development.

Overall, and for all the five plant's life stages that were modeled here, vegetation typically leaded to an increase in the degree of braiding and mean height of the bars (Figure 13a), deeper channels and scour holes (Figures 9 and 13b) and to a reduction of channel mobility (Figure 11), relatively to the unvegetated experiment. However, the influence of flow magnitude decreased as vegetation strength augmented, to increase again in presence of dried vegetation.

4.3 | Effects of low-bedload (deficit) floods

The limitation of sediment supply within the inflow (reduced to 20% of the equilibrium sediment load) that was used in a few selected floods during the present experiments, modelled that case in nature where a large flood removes sediment from the bed, so that the following small flood has a deficit in sediment. During these deficit flood events the river responded by slightly reducing the

number of channels, with some flow paths being abandoned. This trend was reflected by the decrease in topographic regularity values measured by the coefficient α during the deficit floods as shown by Figure 15. Although these low-bedload flows were low magnitude flood events, they presented the same values of α as the high magnitude events. This observation suggests that the feedbacks between bed morphology and vegetation might be stronger in floods with bedload discharges close to equilibrium. Further, in presence of riparian vegetation it is expected that flow resistance will not remain constant as discharge changes. An increase in the discharge during the high floods will lead to a decrease in flow resistance for the same plant size. A deficit in bed load within the floods might also cause a decrease in the shear velocity and hence decreasing flow resistance in those flows, as mentioned by Ma & Huang (2016). Thus, the low-magnitude deficit flood in this study would be expected to act similarly than the high-magnitude equilibrium flood event, as was shown in the results.

The trend in re-establishing the state of dynamic equilibrium (i.e., with the longitudinal bed profile settled around the equilibrium bed slope of 0.015 m/m) modified by previous deficit flood events indicated that effects of such occasional perturbations on the sediment load were smoothed out by the following equilibrium flood, and so that, in the long term. This might be not true when a deficit flood is followed immediately by further deficit flood events, causing a greater impact and effectively a reduction in the equilibrium slope, and therefore channel incision and reduction in the effective width of the system. Deeper channels (higher banks due to incision) will also likely to reduce the lateral channel mobility. Further, the presence vegetation during the deficit flood in Run 13 suggested that mature plants

might lead to greater scour depths, and without a period of recovery, might induce irreversible changes in the long-term morphodynamic development of the river.

Finally, the sediment storage behind vegetation only declined in two occasions: during the few arbitrary deficit floods and during the drought conditions to the end of the experiment (Stage 5). In the first scenario, the low-bedload floods notably removed the sediment stored behind the vegetation patches denoting the impact of the absence of plant colonisation. Therefore, without the advance of the plants between floods and thus, the re-colonisation of the stored sediment, the deposits were not protected by the flexible aboveground biomass or by the root system, and the sediment stored by previous floods was easily removed by the deficit floods (Figure 4). Second, in the drying scenario of Stage 5, the dried plants facilitated the liberation of the excess sediment, locally aggraded behind the vegetation, and leaded to an increase in the sediment being delivered at the downstream end of the rivers. Hence, deficit floods or floods following an extended drought with stressed vegetation might generate an oversupply of sediment to downstream river reaches.

5 | Conclusions

This paper has presented experimental data detailing the changes to the river morphodynamics due to short-term flow variability over different riparian vegetation life stages. Three principal conclusions can be drawn from this work:

1. The presence of vegetation, in absence of plant colonisation, leads to an increase in the number of channels (BI) and topographic irregularity (computed by the coefficient α) relative to the unvegetated condition.

This enhancement of channel development by the vegetation is most noticeable during the low-magnitude flood events (higher relative submergence) due to the braidplain vegetation diverting the flow. This increase in the number of channels is accompanied by a declining trend in the degree of confinement by vegetation.

2. The vegetation life stages play a major role in controlling the impact of the introduced hydrograph on channel morphodynamics. Changes in morphology are more sensitive to flow variability in the presence of younger stage vegetation (in which rooting depths are substantially less than channel depths, i.e., Stage 1) and also when vegetation is in decay (during drought conditions in Stage 5). As the vegetation grows (Stages 2-4), changes in channel morphology (number of channels) are less sensitive and less dependent on flow magnitude. In this context, as smaller flood events are less likely to remove vegetation (in particular, during Stage 1 with the pioneer vegetation), smaller flood events that precede larger events will have lower velocities and would be expected to produce less erosion than if the same smaller flood event followed a high-magnitude event. It is therefore concluded that flood sequencing can be an important driver of geomorphic change depending on the vegetation cycles and should be consider in modelling efforts.
3. Deficit floods (floods with low bed load discharge rates), reduce the interaction between plants and morphology, and cause smaller magnitude flood events to produce channel changes that are comparable to larger flood events with equilibrium bed load discharge rates.

This study advances the understanding of river-vegetation interactions under flow variability (flood sequencing) in order to be able to produce more accurate long-term (decade scale) modelling of the process-response of braiding systems to a raise in the frequency of hydrologic events.

6 | Acknowledgements

The work described in this publication was supported by the European Community's Horizon 2020 Programme through the grant to the budget of the Integrated Infrastructure Initiative HYDRALAB+, Contract nº 654110. D. Parsons also acknowledges funding from the Horizon 2020 ERC Programme (Geostick 78525). Special thanks go to Brendan Murphy for providing invaluable assistance in the setup and performing of the experiments. During this study, R. Fernandez was on research leave from the National Scientific and Technical Research Council, Argentina.

7 | References

Arscott, D., Tockner, K., van der Nat, D. & Ward, J. (2002). Aquatic habitat dynamics along a braided alpine river ecosystem (Tagliamento river, Northeast Italy). *Ecosystems*, 5, 802-814.

Ashmore, P. & Parker, G. (1983). Confluence scour in coarse braided streams. *Water Resources Research*, 19, 392-402.

Bätz, N.(2016). Understanding braided river landform development over decadal time scale: soil and groundwater as controls on biogeomorphic succession. PhD thesis, University of Lausanne, pp. 237. http://serval.unil.ch.

Baynes, E. R. C., van de Lageweg, W. I., McLelland, S. J., Parsons, D. R., Aberle, J., Dijkstra, J., … Moulin, F. (2018). Beyond equilibrium: Re-evaluating physical modelling of fluvial systems to represent climate changes. *Earth-Science Reviews*, 181, 82-97. doi: 10.1016/j.earscirev.2018.04.007.

Best, J. L. (1986). The morphology of river channel confluences. *Progress in Physical Geography*, 10, 157-174.

Bridge, J. S. (1993). The interaction between channel geometry, water flow, sediment transport and deposition in braided rivers. In: *Braided Rivers*, Best, J., & Bristow, C. (Eds.), Nº75, London, 13-71.

Bristow, C. S. & Best, J. L. (1993). Braided rivers: perspectives and problems. In: *Braided Rivers*, Best, J., & Bristow, C. (Eds.), 75, London, 1-11.

Brodu, N. & Lague, D. (2012). 3D Terrestrial lidar data classification of complex natural scenes using a multi-scale dimensionality criterion: applications in geomorphology. Geosiences Rennes. arXiv:1107.0550v3.

Corenblit, D., Tabacchi, E., Steiger, J. & Gurnell, A.M. (2007). Reciprocal interactions and adjustments between fluvial landforms and vegetation dynamics in river corridors: A review of complementary approaches. *Earth-Science Reviews* 84, 56-86. doi:10.1016/j.earscirev.2007.05.004.

Corenblit, D., Steiger, J., Gurnell, A.M., Tabacchi, E. & Roques, L. (2009). Control of sediment dynamics by vegetation as a key function driving biogeomorphic succession within fluvial corridors. *Earth Surface Processes and Landforms* 34, 1790 -1810. doi:10.1002/esp.1876.

Corenblit, D., Steiger, J., Gonzalez, E., Gurnell, A.M., Charrier, G., Darrozes, J., Dousseau, J., Juline, F., Lambs, L., Larrue, S., Roussel, E., Vautier, F. &

Voldoire, O. (2014). The biogeomorphological life cycle of poplars during the fluvial biogeomorphological succession: a special focus on Populus nigra L. *Earth Surface Processes and Landforms* 39, 546-567. doi: 10.1002/esp.3515.

Coulthard, T. (2005). Effects of vegetation on braided stream pattern and dynamics, *Water Resources Research*, 41(4). doi.org/10.1029/2004WR003201.

Crouzy, B., Edmaier, K., Pasquale, N. & Perona, P. (2013). Impact of floods on the statistical distribution of riverbed vegetation. *Geomorphology*, 202, 51-58. doi: 10.1016/j.geomorph.2012.09.013.

Chen, Z., Ortiz, A., Zong, L. J. & Nepf, H. (2012). The wake structure downstream of a porous obstruction with implications for deposition near a finite patch of emergent vegetation, *Water Resour. Res.*, 48, W09517. doi:10.1029/2012WR012224.

Egozi, R. & Ashmore, P. (2008). Defining and measuring braiding intensity. *Earth Surface Processes and Landforms*, 33, 2121-2138. doi: 10.1002/esp.1658.

Follett, E. M. & Nepf, H. M. (2012). Sediment patterns near a model patch of reedy emergent vegetation, *Geomorphology*, 179, 141- 151. doi:10.1016/j.geomorph.2012.08.006.

Garssen, A.G., Verhoeven, J. & Soons, M. (2014). Effects of climate-induced increases in summer drought on riparian plant species a meta-analysis. Freshwater Biology, 59(5): 1052-1063. doi: 10.1111/fwb.12328.

Gran, K. & Paola, C. (2001). Riparian vegetation controls on braided stream dynamics. Water Resources Research, 37(12), 3275-3283.

Gurnell, A. M., Petts, G. E., Harris, N., Ward, J., Tockner, K., Edwards, P. & Kollmann, J. (2000). Large wood retention in river channels: the case of the Fiume Tagliamento, Italy. *Earth Surf. Processes Landforms*, 25, 255–275.

Gurnell, A. M., Petts, G. E., Hannah, D. M., Smith, B. P. G., Edwards, P. J., Kollmann, J., Ward, J. V. & Tockner, K. (2001). Riparian vegetation and island formation along the gravel-bed Fiume Tagliamento, Italy, *Earth Surf. Processes Landforms*, 26, 31–62.

Gurnell, A. & Petts, G. (2006). Trees as riparian engineers: the Tagliamento River, Italy. *Earth Surface Processes and Landforms*, 31, 1558-1574.

Gurnell, A., Blackall, T. D. & Petts, G. E. (2008). Characteristics of freshly deposited sand and finer sediments along an island-braided, gravel-bed river: The roles of water, wind, and trees, *Geomorphology*, 99(1-4), 254-269.

Holloway, J. V., Rillig, M. C., & Gurnell, A. M. (2017). Physical environmental controls on riparian root profiles associated with black poplar (Populus nigra L.) along the Tagliamento River, Italy. *Earth Surface Processes and Landforms*, 42(8), 1262-1273. doi:10.1002/esp.4076.

Hoyle, J., Hicks, M., Stecca, G., Fedrizzzi, D. & Tal, M. (2017). The effects of vegetation in braided rivers. Braided 2017 Symposium, New Zealand.

Hupp, C. & Bornette, G. (2003). Vegetation as a Tool in the interpretation of fluvial geomorphic processes and landforms in humid temperate areas. Chapter in *Tools in Fluvial Geomorphology*. Edited by G. Kondolf and H. Piégay. ISBN:0-471-49142-X.

IPCC, 2014: Climate Change 2014: Synthesis Report. Contribution of Working Groups I, II and III to the Fifth Assessment Report of the Intergovernmental

Panel on Climate Change, Geneva, Switzerland, 151 pp. doi:10.1017/CBO9781107415324.004.

Johnson, W. C. (1994). Woodland expansion in the Platte River, Nebraska: Patterns and causes. *Ecological Monographs*, 64,45-84.

Johnson, W. B., Sasser, C. E. & Gosselink, J. G. (1985). Succession of vegetation in an evolving river delta, Atchafalaya Bay, Louisiana. *Journal of Ecology* 73, 973-986.

Landon, N., Piégay, H. & Bravard, J. (1998). The Drome River incision (France): from assessment to management. *Landscape Urban Plann*. 43, 119-131.

Le Bouteiller & Venditti, C. J. G. (2015). Sediment transport and shear stress partitioning in a vegetated flow. *Water Resources Research,* 51. doi:10.1002/2014WR015825.

Luhar, M. & Nepf, H. (2013). Flow-induced reconfiguration of buoyant and flexible aquatic vegetation. *Limnology and Oceanography*, 56(6), 2003-2017.

Meyer-Peter, E. & Müller, R. (1948). Formulas for Bed-Load Transport. *Proceedings 2nd Congress International Association of Hydraulic Research*, Stockholm, 39-64.

Millar, R.G. (2000). Influence of bank vegetation on alluvial channel patterns. *Water Resources Research*, 36, 1109-1118.

Mosley, M. (1976). An experimental study of channel confluences. *Journal of Geology*, 84, 535-562.

Naiman, R.J., Elliott S.R., Helfield, J.M. & O'Keefe, T.C. (1999). Biophysical interactions and the structure and dynamics of riverine ecosystems: the

importance of biotic feedbacks. Hydrobiologia 410, 79–86. doi: 10.1023/A:1003768102188.

Nepf, H. M. (2012). Hydrodynamics of vegetated channels. *Journal of Hydraulic Research*, 50(3), 262-279. doi: 10.1080/00221686.2012.696559.

Nepf, H.M. (1999). Drag, turbulence, and diffusion in flow through emergent vegetation. *Water Resources Research*, 35(2), 479-489.

Paola, C. (2001). Modelling stream braiding over a range of scales. In *Gravel bed rivers V*. Mosley, M.P. (Eds.), New Zealand Hydrologic Society, Wellington, 11-46.

Parker, G., Wilcock, P., Paola, C., Dietrich, W. & Pitlick, J. (2007). Physical basis for quasi-universal relations describing bankfull hydraulic geometry of single-thread gravel bed rivers. *Journal of Geophysical Research*, 112, F04005. doi: 10.1029/2006JF000549.

Peakall, J., Ashworth, P. & Best, J. (1996). Physical modelling in fluvial geomorphology: principles, applications and unresolved issues. The scientific nature of geomorphology, *Proceedings of the 27th Binghamton symposium in geomorphology*, Rhoads, B. and Thorn, C. (Eds.), 9, 221-253.

Piégay, H. & Gurnell, A.M. (1997). Large woody debris and river geomorphological pattern: examples from S.E. France and S. England. *Geomorphology* 19, 99-116. doi: 10.1016/S0169-555X(96)00045-1.

Piégay, H., Alber, A., Slater, L. & Bourdin, L. (2009). Census and typology of braided rivers in the French Alps. *Aquatic Sciences*, 71, 371-388. doi:10.4319/lo.2011.56.6.2003.

Pittaluga, M., Coco, G. & Kleinhans, M. (2014). A unified framework for stability of channel bifurcations in gravel and sand fluvial systems. *Geophysical Research Letters*, 42, 7521-7536. doi:10.1002/2015GL065175.

Redolfi, M., Tubino, M., Bertoldi, W. & Brasington, J. (2016). Analysis of reach scale elevation distribution in braided rivers: Definition of a new morphologic indicator and estimation of mean quantities, *Water Resources* Research, 52, 5951-5970. doi: 10.1002/2015WR017918.

Tal, M. & Paola, C. (2007). Dynamic single-thread channels maintained by the interaction of flow and vegetation. *Geology*, 35(4), 247-350. doi: 10.1130/G23260A.1.

Tal, M. & Paola, C. (2010). Effects of vegetation on channel morphodynamics: results and insights from laboratory experiments. *Earth Surface Processes and Landforms,* 35 (9),1014-1028. doi: 10.1002/esp.1908.

Tal, M., Gran, K., Murray, A., Paola, C. & Hicks, D. (2004). Riparian vegetation as a primary control on channel characteristics in multi-thread rivers. In: *Riparian Vegetation and Fluvial Geomorphology*, Water Sci. Appl. Ser., vol. 8, Bennett and Simon, A. (Eds.), 43-58, AGU, Washington, D. C.

Toffolon, M. & Crosato, A. (2007). Developing macroscale indicators for estuarine morphology: The case of the Scheldt Estuary, *Journal of Coastal Research*, 23(1), 195-212, doi: 10.2112/03-0133.1.

Toone, J., Rice, S. & Piégay, H. (2014). Spatial discontinuity and temporalevolution of channel morphology along a mixed bedrock-alluvial river,upper Drôme River, southeast France: Contingent responses to external and internal controls. *Geomorphology*, 205, 5-16.

Yang, H., Kin, B., Sun, J. & Huang, G. (2017). Simulating laboratory braided rivers with bed-load sediment transport. *Water*, 9, 686. doi : doi:10.3390/w9090686.

Yuanxu Ma & He Qing Huang. (2016). Controls of channel morphology and sediment concentration on flow resistance in a large sand-bed river: A case study of the lower Yellow River. *Geomorphology*, 264, 132-146. doi: org/10.1016/j.geomorph.2016.03.035.

Van Dijk, W. M., Teske, R., van de Lageweg, W.I. & Kleinhans, M. (2013). Effects of vegetation distribution on experimental river channel dynamics. *Water Resources Research*, 49(11), 7558-7574. doi: 10.1002/2013WR013574.